Effect of External Force and Bimanual Operation on Upper Limb Pose during Human-Robot Collaboration

Richardo Khonasty, Marc G. Carmichael, Dikai Liu and Stefano Aldini

Abstract

During physical Human-Robot Interaction (pHRI) in industrial applications such as human-robot collaborative abrasive blasting, the operator often interacts with the robot using two hands, exchanging forces through handle bars. For the robot to provide appropriate assistance to the operator and for safe interaction, it would be beneficial for the robot to know the pose of the user. This problem is often challenging due to environmental factors, limited sensing capability in the environment and the robot, and redundancy of the human upper-limb. This paper presents experimental study on how two-hand interaction and force exchange affect the operators upper-limb pose, which can be characterized by swivel angle. The poses of ten subjects were recorded as they interacted with a collaborative robot. Differences in the adopted upper limb pose were analyzed with respect to factors such as unimanual versus bimanual operation, and the amplitude of interaction force between an operator and the robot. The results discovered that the the effect of bimanual operation on the upper limb pose differs between individuals and the magnitude of the force had a varying effect on the pose. The requirement of applying a force forward produced an overall lower swivel angle.

1 Introduction

One reason as to why collaborative robots are gaining interest is due to their capability to utilize human adaptability with robotic strength [Spinelli *et al.*, 2015; Krüger *et al.*, 2009]. An example of this are robots employed to assist human workers by reducing the amount of effort required in tasks [Sylla *et al.*, 2014]. During physical Human-Robot Interaction (pHRI) in industrial applications such as human-robot collaborative abrasive blasting (Figure 1), the operator often interacts with the robot with two hands, exchanging forces through handle bars. To ensure the safety of the user and improve the effectiveness of the robot assistance, it would be beneficial for the robot to know the user's pose. For example, pose estimation of the user in the workspace of the robot would allow the robot to accommodate the human in the robot's collision detection and/or avoidance algorithm. Other influence of the pose on robot behavior would be in intent recognition or in the calculation of human strength through the use of a musculoskeletal model [Holzbaur *et al.*, 2005]. Studies conducted on the capability of a human to exert forces at the hand using musculoskeletal models [Carmichael and Liu, 2013; 2015; Hernandez *et al.*, 2015; 2016] have found that the strength output at the hand is affected by the pose of the upper limb.

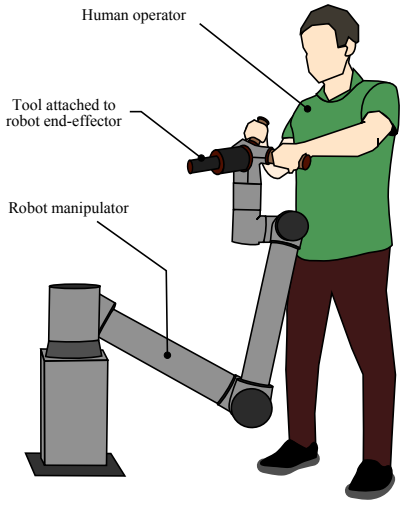

Figure 1: An example scenario: a physical human robot collaborative abrasive blasting

Determining the pose of the human upper limb is often challenging due to environmental factors. These factors include presence of objects that obscure views from the

sensors or unfavorable lighting conditions. Limited sensing capabilities in the environment and lack of sensing from the robot also reduces the amount of information that can be perceived from the user. A large degree of freedom (DOF) and the redundant nature of the human upper limb means that multiple poses exist for a given hand or wrist position. Current solutions to real time measurement of poses is often not practical for many applications. A motion capture system require many cameras placed in a well defined environment to reliably track a person. Marker or Inertial Measurement Unit (IMU) based tracking systems require the user to accurately place sensors or markers on the user's body which is not compatible for real life or industrial applications where protective equipment are commonly used.

Models for predicting upper limb pose have been developed that reduce the need for direct measurement [Soechting *et al.*, 1995; Kim *et al.*, 2012; Li *et al.*, 2013; 2015; Kang *et al.*, 2005]. These models utilized various concepts such as minimizing change in the kinetic energy [Soechting *et al.*, 1995] or maximizing manipulability of the hand towards a point on the head [Kim *et al.*, 2012]. Upper limb prediction models are often developed based on a free unconstrained operator conditions.

In a pHRI scenario, such as the one shown in Figure 1, it cannot be assumed that the human will be able to move freely. By having the robot in the physical proximity of the human several constraints are placed on the poses that the human is able to undertake. The robot may be controlled through physical interaction by applying forces through an interface such as a handle. Factors such as the handle positions and orientations prescribes the relative distance between hands, which was found to alter force output capabilities [Lin *et al.*, 2012]. Having a predefined handle dictates the orientation of the wrist, which has been shown to alter the adopted pose of the user [Kim and Rosen, 2015]. In tasks where the human is required to exert forces, the adopted pose may be altered to account for the forces that needs to be supplied. This paper presents and investigation on the significance of interaction forces and bimanual operation on the human pose adopted during interaction with a robot.

2 Upper Limb Pose Definition

The human upper limb has a large range of motion which allows humans to naturally adopt a comfortable pose for a specific hand position. The upper limb is often approximated as a system with 7 DOF, consisting of a 3 DOF shoulder, 1 DOF elbow and 3 DOF wrist. This results in a 1 DOF redundancy when the position and orientation of the hand is defined. One parameterization of this redundancy is called the swivel angle ϕ [Tolani and Badler, 1996]. Utilizing the swivel angle, the configuration of the upper limb can be defined alongside the position $[P_{WX}, P_{WY}, P_{WZ}]$ and orientation $[R_{WX}, R_{WY}, R_{WZ}]$ of the wrist relative to the shoulder (Equation 1).

$$pose = [P_{WX}, P_{WY}, P_{WZ}, R_{WX}, R_{WY}, R_{WZ}, \phi] \quad (1)$$

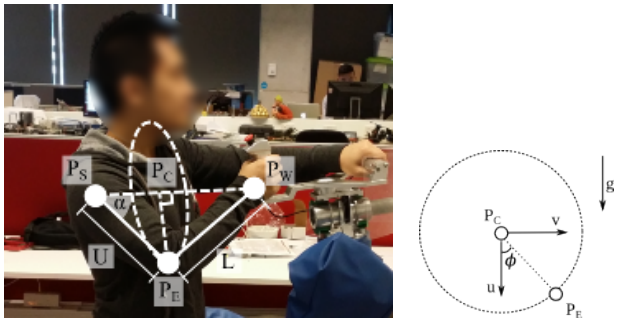

(a) (b)

Figure 2: a) Location of the swivel coordinate frame P_C in relation to the subject's shoulder P_S, elbow P_E and wrist P_W b) Swivel coordinate frame $\vec{u} \times \vec{v}$ showing the swivel angle ϕ and direction of gravity $\vec{g}$.

$$P_C = P_S + U\cos(\alpha) \quad (2)$$
$$\cos(\alpha) = \frac{L^2 - U^2 - ||P_W - P_S||}{2U||P_W - P_S||}$$

$$P_E = R[cos(\phi)\vec{u} + sin(\phi)\vec{v}] + P_C \quad (3)$$
$$R = U\sin(\alpha)$$

$$\vec{n} = \frac{(P_W - P_S)}{||P_W - P_S||}, \quad \vec{u} = \frac{\vec{g} - (\vec{g}\cdot\vec{n})\vec{n}}{\vec{g} - (\vec{g}\cdot\vec{n})\vec{n}}, \quad \vec{v} = \vec{n} \times \vec{u} \quad (4)$$

The swivel angle ϕ refers to the angle relative to an imaginary coordinate frame positioned along a vector between the wrist and the shoulder on the point P_C. P_C can be calculated using the position of the shoulder P_S, the position of the wrist P_W, and the length of the upper and lower arm, U and L respectively (Equation 2). The coordinate frame is located in such a way that the position of the elbow, P_E (Equation 3), lies on the $\vec{u}\vec{v}$ plane where $\vec{u}$ is suggested to be aligned to the direction of gravity $\vec{g}$ (Equation 4) as shown in Figure 2. The swivel angle ϕ of a given upper limb pose can be calculated by determining the angle between $\vec{u}$ and $\overrightarrow{P_C P_E}$.

3 Experimental Method

Experiments were conducted which simulate a collaborative operation between a human operator and an assistive robot which is controlled using one or two handles

at the end effector. A universal robot UR10 was used for all of the experiments (Figure 4). An end effector with two handles was attached to the UR10 with an ATI Mini 45 force/torque sensor placed between the two handles and the tool adapter of the robot. The force/torque sensor was used to capture the magnitude and direction of forces that were applied by the subjects. A ±5N threshold was applied to the specified force in each experiment. If a force was measured above this threshold the robot will halt operation. The robot will resume operation once the force applied by the user is between the applied threshold. A visual aid, shown in Figure 3, was used to display the forces being applied to aid the user in applying the correct magnitude of force. Visual cues dictated the direction in which the force needs to be applied. The visual aid also served as a distraction to the subject, reducing their awareness in the movement of their upper limb, which results in a more natural pose being adopted.

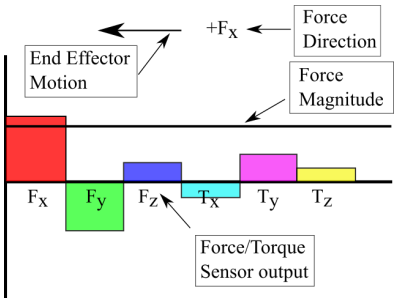

Figure 3: Visual aid used to display current Force/Torque sensor output alongside current experimental requirements such as the magnitude and direction of the force required from the subject and the current end effector motion

The UR 10 robot was programmed to only move its end effector when the force being applied by the subject satisfies the magnitude and directional requirement. The orientation of the end effector was kept constant as it moved along the specified path (Figure 4b). To ensure repeatability and consistency of the upper limb pose measurements between experiments and between subjects, the trajectory of the end effector was determined by the robot. This removes the human error in the path trajectory and allows comparison to be conducted at the same point for the same subject across different experiments or against other subjects. In all of the experiments, the UR10's end effector is moved at 0.1m/s.

Ten healthy subjects performed all six experiments. All subjects were male, heights ranging from 165 cm to 185 cm, with two being left handed. The experiments conducted are covered under UTS ethical approval HREC No:ETH15-0038. Each subject conducted the

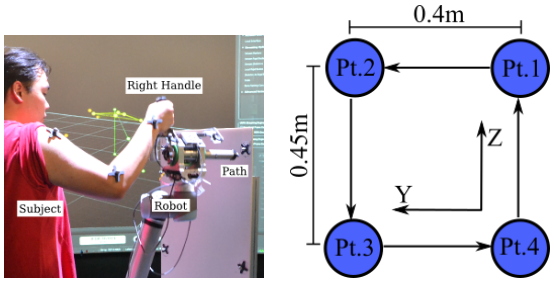

(a) (b)

Figure 4: (a) Experimental setup showing a subject and the UR10 robot used for the experiment (b) Path of the end effector during experiment with the force coordinate system.

.

experiments in a seated position with their back fully rested. Each subjects were asked to minimize the movement of their torso througout the experiment. The placement of the seat for each subject was adjusted such that the subjects never reach their full reach. When the arm is fully stretched, the calculation of the swivel angle becomes inaccurate. The location of the seat were kept constant throughout all experiments for the single subject. After each experiment, the volunteers are given a short break to ensure that fatigue had a minimal effect on the pose recorded.

Several experiments were conducted to observe the pose that is adopted by the human upper limb under different conditions or constraints. Experiments were chosen to test the effect of the different conditions such as whether one or two hands were used during the operation or the magnitude of the force that the subject had to apply during the experiment. The experiments conducted were:

- Experiment 1: 1 hand, with no force applied by user (1 Hand, 0N force)
- Experiment 2: 2 hands, with no force applied by user (2 Hands, 0N force)
- Experiment 3: 1 hand, with 20N force being applied along the direction of the task (1 Hand, 20N force, +X)
- Experiment 4: 1 hand, with 40N force being applied along the direction of the task (1 Hand, 40N force, +X)
- Experiment 5: 1 hand, with 20N force being applied along the direction of motion (1 Hand, 20N force, YZ Plane)
- Experiment 6: 1 hand, with 40N force being applied along the direction of motion (1 Hand, 40N force, YZ Plane)

In one handed (Unimanual) experiments, the right hand of the subject is used to hold the specified handle (Figure 4a) and apply as little force as possible. This experiment is designed to act as the baseline to which other experimental results are compared against. Experiment 2 requires the user to place both hands (Bimanual) onto the end effector at specified handle locations. This experiment will be used to determine if the addition of the left hand will change the pose adopted by the right limb. Experiments 3 to 6 require the user to apply a force of either 20N or 40N in magnitude in a specified direction with little to no force in the other directions. For the force direction, the coordinate system in Figure 4b was used. In Experiments 3 and 4 the specified direction is along the nozzle of the end effector, +X (into the page). These experiments were designed to determine the effect of pushing against a load to the pose adopted by the subjects. The increased force in Experiment 4 was chosen to determine whether an larger force further increased the change in the upper limb pose. In Experiments 5 and 6 the force is to be applied in the direction of end effector motion. For example, between Pt 2 and Pt 3 the specified force direction is in the -Z direction. These experiments were designed to simulate moving a heavy object or a slow responding end effector.

4 Data Collection

Reflective markers are attached to each subject's shoulder, elbow and wrist to observe the adopted pose of the upper limb. Markers are also attached to the end effector of the robot to track the user's progress (Figure 4a). The upper limb poses were recorded using an Optitrack motion capture system which used 12 Optitrack Prime 17 W cameras placed 3 m above the ground and evenly spaced around a 10 m diameter motion capture lab. The data was collected at 120 frames per second.

4.1 Swivel Angle Calculation

The data obtained from the Optitrack system were used to calculate the swivel angle at each time step. The full pose of the upper limb were calculated by finding the angle ϕ between the two vectors, $\vec{u}$ and $\overrightarrow{P_C P_E}$ (Equation 3). In each experiment a mean and standard deviation of the swivel angle were calculated at specific end effector points along the path. A comparison was then conducted using the mean swivel angle obtained in Experiment 1 against data obtained in the other experiments. Experiment 1 was chosen to be the baseline for comparison as the subject is under no load other than gravity whilst still constrained by the robot for the position and orientation of their hands. The swivel angle recorded for each subject during Experiment 1 were also compared to determine variability across the subject cohort.

5 Result & Discussion

5.1 Experiment 1 - Unimanual Operation with No Force Applied

To increase consistency of the result, each experiment was repeated 6 times with each loop starting and ending at Point 1. For every upper limb pose recorded in the experiments, a swivel angle was calculated. These swivel angles were grouped to specific end effector positions along the path. For each of these groups, a mean and standard deviation value was calculated. Figure 5a shows the mean and standard deviation of the swivel angle in Experiment 1 for an individual subject. In Figure 5, the horizontal axes corresponds to the distance traveled by the end effector throughout the experiment. The vertical axes represents the calculated swivel angle. Figure 5b shows the mean value of the swivel angles for all ten subjects.

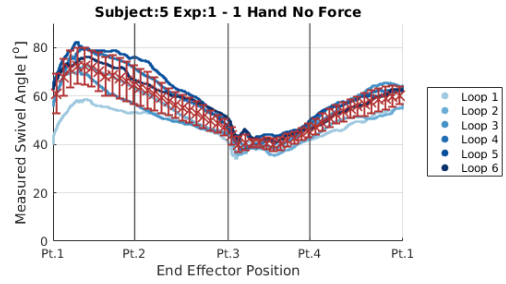

(a)

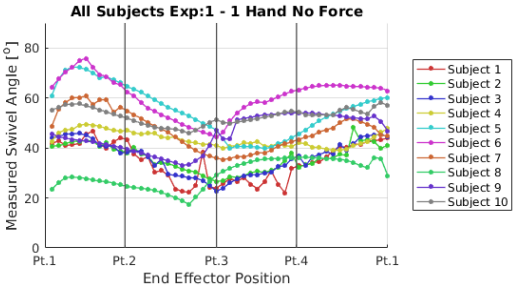

(b)

Figure 5: (a) Swivel angles calculated in Experiment 1 from subject 5, (b) Mean swivel angles of all 10 subjects in Experiment 1

From Figure 5a it can be seen that the swivel angle for a given subject is repeatable with slight deviations. This repeatability is also seen across the cohort. For each of the 10 subjects the mean swivel angle at specified end effector positions were calculated (Figure 5b). The mean swivel angle values from Experiment 1 (Figure 5b) will be used as the baseline for comparison with the swivel angles from other experiments by the same subject.

To compare the difference in the calculated swivel angles between subjects, a Root Mean Square Deviation (RMSD) was used. Table 1 shows the RMSD for each of

the subject in Experiment 1. Each value was calculated using one subject's baseline compared to their own or another subject's swivel angles throughout Experiment 1.

In Experiment 1, it can be seen that the swivel angles calculated along the same path is quite repeatable (Figure 5a). Data obtained from other subjects also reflect this trend. When compared to their own data, the RMSD values is the smallest (Table 1). Figure 5b and Table 1 shows that from the data collected, every subject naturally adopts a different pose to perform a similar motion. Results from Experiment 1 suggests that an upper limb prediction model should be individualized to obtain a higher accuracy.

5.2 Experiment 2 - Bimanual Operation with No Force Applied

In Experiment 2, each subject was tasked with applying as little force as possible whilst holding onto the end effector with both hands. Similar to results found in Experiment 1, the calculated swivel angles in Experiment 2 were quite repeatable. Figure 6 shows the mean swivel angles which shows that each subject performed the Experiment 2 in a different manner.

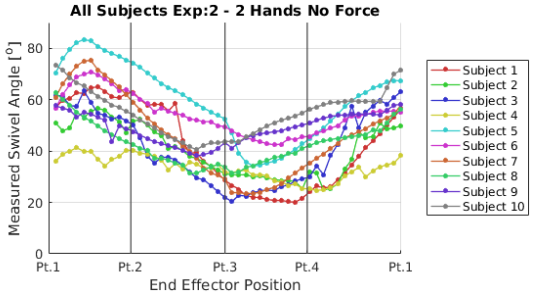

Figure 6: Mean swivel angles of all 10 subjects in Experiment 2

A comparison was conducted on the difference that was observed between swivel angles calculated in Experiment 1 and 2. Figure 7 shows a plot of the mean and standard deviation of the swivel angle calculated for subject 5 in Experiment 1 and 2. The overall trend across all subject shows that there is a slight change in the calculated swivel angle in Experiment 2. Observable effects to the swivel angle differ between subjects. Several subjects maintained a similar swivel angle to Experiment 1 with changes only occurring surrounding Pt 1 of the experimental path, such as in Figure 7.

The effect of bimanual operation to the swivel angle is difficult to ascertain from the results obtained in the ten subjects. It is hypothesized that the bimanual operation will affect the pose adopted by the user especially when one of the arms is closer to it's limit. This trend was

Figure 7: Comparison of the mean swivel angles for Experiment 2 and Experiment 1

able to be seen in seven out of the ten subjects where the largest difference in the swivel angle was observed around Pt 1 where the left arm is close to its full reach. The standard deviation of the swivel angle between Pt 3 and Pt 4 of the path is smaller in comparison to the other sections of the experimental path. This is likely due to the right arm being close to it's full reach at this area.

5.3 Experiments 3 and 4 - Unimanual Operation with 20N or 40N Task Load

Experiments 3 and 4 required the subject to apply 20N or 40N. The direction of the force was chosen to mimic a sandblasting task where a load is applied by the operator along the direction of the end effector's nozzle and away from the torso. Similar to findings in previous experiments, the calculated swivel angle in Experiments 3 and 4 were repeatable for each subject and a larger variability observed across subjects (Figure 8a and 8b).

Figure 9a and 9b shows the comparison of the swivel angle calculated for the respective experiments against the swivel angle calculated for Experiment 1. From the calculated swivel angles of all ten subjects, it was found that the swivel angles in Experiments 3 and 4 were lower in value when compared to the swivel angles from Experiment 1. Seven of the ten subjects presented a lower swivel angle in Experiment 4 when compared to Experiment 3 but others was observed to have a higher overall swivel angle. It was hypothesized that the lower swivel angle allows the human body to exert a larger force in the forward direction.

5.4 Experiments 5 & 6 - Unimanual Operation with 20N or 40N Interaction Load

In these two experiments, each subject was asked to apply forces of either 20N or 40N in magnitude. The direction of the forces is altered to match the direction of travel of the end effector.

In Experiment 5, four subjects were observed to perform the experiment in a similar manner to Experiment 1

		Calculated Swivel Angles									
		Sub 1	**Sub 2**	**Sub 3**	**Sub 4**	**Sub 5**	**Sub 6**	**Sub 7**	**Sub 8**	**Sub 9**	**Sub 10**
Mean Swivel Angle	**Sub 1**	4.97	6.08	5.69	9.93	21.08	26.19	13.98	10.04	12.87	18.34
	Sub 2	6.42	4.57	5.07	8.83	19.80	24.90	12.78	9.54	11.18	17.06
	Sub 3	6.07	5.34	4.34	8.79	19.62	24.71	12.58	10.02	11.33	16.87
	Sub 4	10.96	9.49	9.49	3.50	13.11	17.57	8.86	14.50	9.81	9.86
	Sub 5	21.43	19.91	19.52	13.14	5.00	9.41	10.48	25.90	16.20	9.11
	Sub 6	26.67	24.99	24.77	17.51	10.31	4.28	15.24	31.15	16.06	9.23
	Sub 7	13.80	12.15	11.85	7.17	9.71	14.28	5.96	18.01	11.61	8.04
	Sub 8	10.86	10.26	10.56	14.66	26.05	31.22	18.97	3.49	16.86	23.38
	Sub 9	13.94	11.82	11.92	9.45	15.81	15.58	12.27	16.61	4.35	8.40
	Sub 10	19.14	17.50	17.28	10.03	10.04	9.61	9.96	23.45	9.71	2.94

Table 1: Root Mean Square Deviation (RMSD) comparison of a subject's mean swivel angle against swivel angles of all subjects calculated for Experiment 1

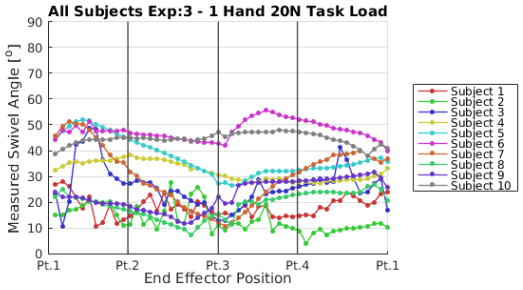

(a) Mean swivel angles for all 10 subjects for Experiment 3

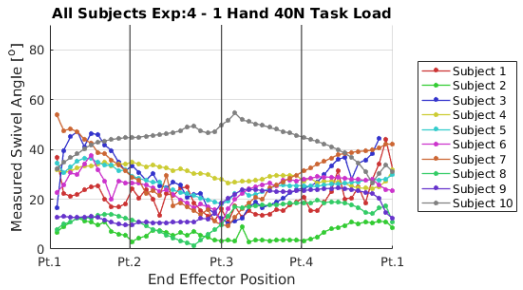

(b)

Figure 8: Mean swivel angles for all 10 subjects for: (a) Experiment 3, (b) Experiment 4

(a)

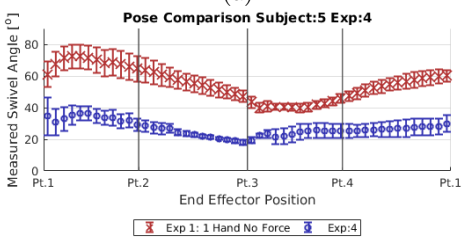

(b)

Figure 9: Comparison of the mean swivel angles for Experiment 1 and (a) Experiment 3, (b) Experiment 4

(Figure 11a), where no load was exerted by the subjects. Four other subjects had a higher overall swivel angle and the last two subjects had a lower overall swivel angle. In Experiment 6, several subjects had difficulty in directing the force to the specified directions. This resulted in a large shift in their upper limb pose such that the force is exerted in the right direction. The variation in the swivel angle is visible in Figure 11b where large shifts was observed between Pt 1 and Pt 2 and between Pt 3 and Pt 4.

5.5 Summary of Each Individual

Table 2 highlights the difference between the swivel angles for each subject. Each column in the table shows the calculated RMSD of the subject's swivel angle when compared against the mean swivel angle calculated in Experiment 1. RMSD values obtained for the same experiment were not consistent between subjects. This further highlights that each individual had a different observed reaction to the factors being considered in this paper.

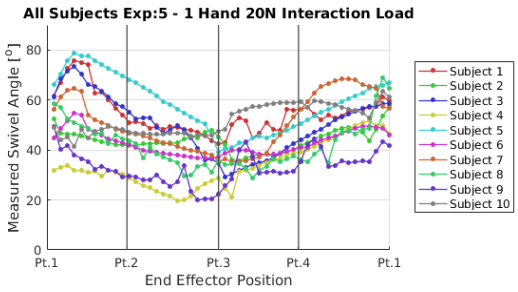

(a) Mean swivel angles for all 10 subjects for Experiment 3

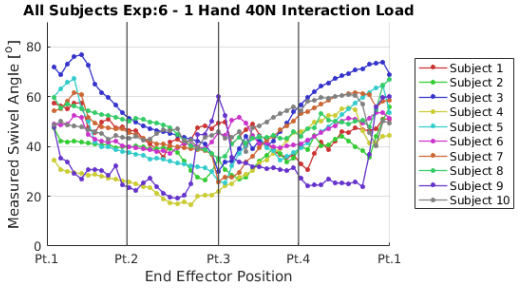

(b)

Figure 10: Mean swivel angles for all 10 subjects for: (a) Experiment 5, (b) Experiment 6

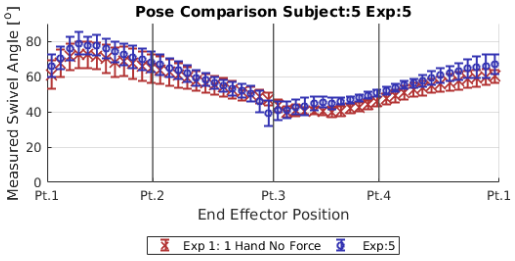

(a)

(b)

Figure 11: Comparison of the mean swivel angles for Experiment 1 and (a) Experiment 5, (b) Experiment 6

6 Strength Comparison using a Musculoskeletal Model

To investigate the trend of a lower swivel angle observed in Experiments 3 and 4, a musculoskeletal model was used to estimate the strength of subject 5. It was speculated that subjects had some form of biomechanical advantage with a lower swivel angle and hence would adopt it when required to exert force at the hand. An upper limb model [Holzbaur *et al.*, 2005] was used in the OpenSim software [Delp *et al.*, 2007] to estimate the maximum opposable strength at the hand. Experiments 1 and 4 were chosen as the two scenario to be compared. Experiment 1 represents a case where the subject performed the task with minimal force interaction. Experiment 4 represented a case where the subject was tasked with applying a large load in the forward direction. These two experiments resulted in a different pose being adopted by the user and it is expected that the strength of the subject is different in these two experiments.

	Exp 2	Exp 3	Exp 4	Exp 5	Exp 6
Sub 1	13.37	17.83	17.41	22.34	14.14
Sub 2	7.96	25.81	29.43	9.27	8.75
Sub 3	9.22	14.08	9.32	14.51	19.67
Sub 4	11.31	11.86	14.00	14.36	16.28
Sub 5	7.25	18.72	28.75	6.31	14.91
Sub 6	10.26	15.60	35.66	17.84	17.00
Sub 7	8.25	16.95	18.87	8.88	8.70
Sub 8	13.98	11.83	16.87	17.53	21.48
Sub 9	7.11	24.45	28.80	18.03	22.68
Sub 10	6.38	8.52	11.15	6.74	9.34

Table 2: Root Mean Square Deviation (RMSD) of the swivel angles in different experiments, measured against the baseline of the same individual

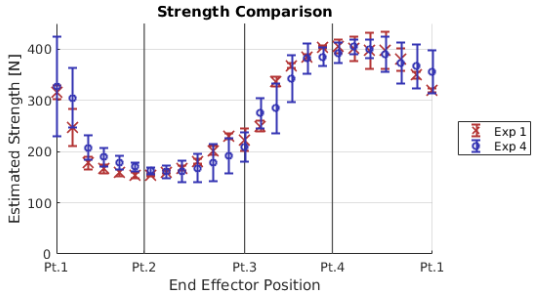

Figure 12: Maximum opposable force of the user during Experiment 1 and Experiment 4

Figure 12 shows the mean and standard deviation of the maximum opposable force at the hand of subject 5 for upper limb poses adopted in Experiments 1 and 4. The mean values of the maximum opposable force were shown to have little in variation and all values are greater than the 40N specified in Experiment 4. In Experiment 1 the calculated standard deviation of the maximum opposable force is on average smaller than those in Experiment 4. It is hypothesized that the increase

in the standard deviation is likely due to the subject's pose altering due to fatigue whereas in Experiment 1 the maximum opposable force were consistent due to the low strength requirement of the task.

7 Conclusion

From the experimental results collected on the pose adopted by ten subjects, it was found that for each subject the swivel angle was observed to be repeatable with small variation. The variation was significantly larger when comparing swivel angle across subjects for the same experiment The calculated swivel angle does not remain consistent when comparing two different subjects. The effect of bimanual operation on the upper limb pose differs between individuals. When the user is tasked with applying a force forward, it was found that the magnitude of the force had a varying effect on the pose. The requirement of applying a force forward produced an overall lower swivel angle. The magnitude of the force had a larger impact in the adopted pose during the experiments where the direction of the force to be applied is aligned to the path of the experiment. This suggests that the direction of the human-robot interaction force and magnitude is an important factor on how it affects the operator's pose. Subjects were found to alter their pose significantly to be able to apply a force in certain directions. Performing maximum opposable strength calculation for Experiments 1 and 4 using a musculoskeletal model shows that the subject had a similar strength profile even with the change in the swivel angle.

8 Acknowledgements

This work is supported in part by the Australian Research Council (ARC) Linkage Project (LP140100950), Burwell Technologies, an Australian Government Research Training Program (RTP) Scholarship and the Centre for Autonomous Systems (CAS) at the University of Technology Sydney. The authors would also like to thank the UTS Data Arena for facilitating the motion capture experiments.

References

[Carmichael and Liu, 2013] Marc G. Carmichael and Dikai Liu. Estimating physical assistance need using a musculoskeletal model. *IEEE Transactions on Biomedical Engineering*, 60(7):1912–1919, 2013.

[Carmichael and Liu, 2015] Marc G. Carmichael and Dikai Liu. Upper limb strength estimation of physically impaired persons using a musculoskeletal model: A sensitivity analysis. *Proceedings of the Annual International Conference of the IEEE Engineering in Medicine and Biology Society, EMBS*, 2015-November:2438–2441, 2015.

[Delp *et al.*, 2007] Scott L. Delp, Frank C. Anderson, Allison S. Arnold, Peter Loan, Ayman Habib, Chand T. John, Eran Guendelman, and Darryl G. Thelen. OpenSim: Open-Source Software to Create and Analyze Dynamic Simulations of Movement. *IEEE Transactions on Biomedical Engineering*, 54(11):1940–1950, nov 2007.

[Hernandez *et al.*, 2015] Vincent Hernandez, Nasser Rezzoug, and Philippe Gorce. Toward isometric force capabilities evaluation by using a musculoskeletal model: Comparison with direct force measurement. *Journal of Biomechanics*, 48(12):3178–3184, 2015.

[Hernandez *et al.*, 2016] Vincent Hernandez, Nasser Rezzoug, Julien Jacquier-Bret, and Philippe Gorce. Human upper-limb force capacities evaluation with robotic models for ergonomic applications: effect of elbow flexion. *Computer Methods in Biomechanics and Biomedical Engineering*, 19(4):440–449, 2016.

[Holzbaur *et al.*, 2005] Katherine R S Holzbaur, Wendy M. Murray, and Scott L. Delp. A model of the upper extremity for simulating musculoskeletal surgery and analyzing neuromuscular control. *Annals of Biomedical Engineering*, 33(6):829–840, 2005.

[Kang *et al.*, 2005] Tao Kang, Jiping He, and Stephen I Helms Tillery. Determining natural arm configuration along a reaching trajectory. *Experimental brain research. Experimentelle Hirnforschung. Experimentation cerebrale*, 167(3):352–361, 2005.

[Kim and Rosen, 2015] Hyunchul Kim and Jacob Rosen. Predicting Redundancy of a 7 DOF Upper Limb Exoskeleton Toward Improved Transparency between Human and Robot. *Journal of Intelligent & Robotic Systems*, 80(S1):99–119, dec 2015.

[Kim *et al.*, 2012] Hyunchul Kim, Levi Makaio Miller, Nancy Byl, Gary M. Abrams, and Jacob Rosen. Redundancy resolution of the human arm and an upper limb exoskeleton. *IEEE Transactions on Biomedical Engineering*, 59(6):1770–1779, 2012.

[Krüger *et al.*, 2009] J. Krüger, T.K. Lien, and A. Verl. Cooperation of human and machines in assembly lines. *CIRP Annals - Manufacturing Technology*, 58(2):628–646, 2009.

[Li *et al.*, 2013] Zhi Li, Jay R yan Roldan, Dejan Milutinović, and Jacob Rosen. The rotational axis approach for resolving the kinematic redundancy of the human arm in reaching movements. *Conference proceedings : ... Annual International Conference of the IEEE Engineering in Medicine and Biology Society. IEEE Engineering in Medicine and Biology Society. Annual Conference*, 2013(2):2507–2510, 2013.

[Li *et al.*, 2015] Zhi Li, Dejan Milutinovic, and Jacob Rosen. Spatial Map of Synthesized Criteria for the Redundancy Resolution of Human Arm Movements. *IEEE Transactions on Neural Systems and Rehabilitation Engineering*, 23(6):1020–1030, 2015.

[Lin *et al.*, 2012] Jia Hua Lin, Raymond W. McGorry, and Chien Chi Chang. Effects of handle orientation and between-handle distance on bi-manual isometric push strength. *Applied Ergonomics*, 43(4):664–670, 2012.

[Soechting *et al.*, 1995] J F Soechting, C A Buneo, U Herrmann, and M Flanders. Moving effortlessly in three dimensions: does Donders' law apply to arm movement? *The Journal of neuroscience : the official journal of the Society for Neuroscience*, 15(9):6271–80, sep 1995.

[Spinelli *et al.*, 2015] Raffaele Spinelli, Giovanna Ottaviani Aalmo, and Natascia Magagnotti. The effect of a slack-pulling device in reducing operator physiological workload during log winching operations. *Ergonomics*, 58(5):781–790, may 2015.

[Sylla *et al.*, 2014] Nahema Sylla, Vincent Bonnet, Frédéric Colledani, and Philippe Fraisse. Ergonomic contribution of ABLE exoskeleton in automotive industry. *International Journal of Industrial Ergonomics*, 44(4):475–481, 2014.

[Tolani and Badler, 1996] D Tolani and N I Badler. Real-time inverse kinematics of the human arm. *Presence (Cambridge, Mass.)*, 5(4):393–401, 1996.